

# Absolute calibration of the Photo-Detector Module of the EUSO-Balloon experiment and improvements for future missions

---

**C. Moretto\***, P. Barrillon, S. Dagoret-Campagne, J. A. Rabanal Reina

*Laboratoire de l'Accélérateur Linéaire, Université Paris-Sud, CNRS/IN2P3*

**S. Bacholle, C. Blaksley, A. Jung, P. Gorodetzky**

*Laboratoire AstroParticule et Cosmologie, Université Paris-Diderot, CNRS/IN2P3*

**S. Blin-Blondil**

*Omega, École polytechnique, CNRS/IN2P3*

**H. Miyamoto**

*Dipartimento di Fisica, Università di Torino and INFN Torino*

## for the JEM-EUSO collaboration

EUSO-Balloon is a balloon borne mission operated by CNES during a one-night flight in August 2014 over the Ontario forest, in Canada, at 38 km altitude. The payload is a technological demonstrator for the Extreme Universe Space Observatory (EUSO) aiming at the detection of Extensive Air Showers (EAS) induced by Ultra High Energy Cosmic Rays (UHECR) from the International Space Station (ISS). The Photo-Detector Module (PDM) of EUSO-Balloon consists of 36 Multi-Anodes Photomultiplier Tubes (MAPMTs) in a square assembly for a total of 2,304 pixels. The characterization at the single photoelectron level in the laboratory has been processed before flight in a dedicated black box. After-flight calibration to check possible decrease of gain and efficiency of the PMTs has been carried out. Finally, we discuss the upgrade of the PDM to improve the gain and the signal-to-noise ratio. The significant progresses made on these aspects represent a first milestone for the R&D of future EUSO-like missions.

*The 34th International Cosmic Ray Conference,*

*30 July- 6 August, 2015*

*The Hague, The Netherlands*

---

\*Speaker.

## 1. Introduction

EUSO-Balloon is a balloon borne pathfinder for the space-based UHECR detector JEM-EUSO [1], a fluorescence detector designed to be placed on the ISS. The EUSO-Balloon mission is led by the French part of the JEM-EUSO collaboration with the support of CNES, the French space agency. The main goals of this pathfinder are:

- Validation of the technologies and components developed for the JEM-EUSO mission by testing the entire acquisition chain through a series of stratospheric balloon flights. Those flights allow also to test the trigger algorithm online or offline, using events generated by cosmic rays or artificial light sources. The latter are generated by laser and flashers that are fired from a helicopter flying below the balloon [2].
- Measuring the UV background [3] from a variety of lands and cloud conditions with an instrument similar to JEM-EUSO. This background light originates from the airglow and star light reflected by Earth or from anthropomorphic sources like cities.

In section 2 the Photo-Detector Module (PDM) of the instrument is presented. Section 3 is devoted to the calibration process. Results are discussed in section 4. The response of the instrument before and after flight is compared. In the final section the improvements that will be applied to the camera in the optics of future flights are discussed.

## 2. Description of the Photo-Detector Module

EUSO-Balloon is a balloon borne fluorescence telescope with a Fresnel optics of about  $1 \text{ m}^2$  to image extensive air showers induced by UHECRs. The detailed description of the optics can be found in [4]. The optics, the PDM, its readout electronics and the data processor are embedded in a mechanical structure (gondola) of almost 3 m height and 1.2 m square basis having a total mass of  $\sim 460 \text{ kg}$ . An overview of the whole detector can be found in [5]. An external infrared camera is also carried by the gondola to monitor the cloud coverage [6].

The PDM is a curved (2.5 m radius) assembly of 36 Hamamatsu M64 MAPMTs of 64 pixels each. The pixel size is 2.88 mm and the total active surface of a MAPMT is about  $23 \times 23 \text{ mm}^2$ . The total number of pixels in the camera is 2,304 for a total surface of  $165 \times 165 \text{ mm}^2$ . MAPMTs are grouped in  $2 \times 2$  square arrays called Elementary Cell (EC). Each EC assembly is powered by the same power supply. The full PDM is thus powered by 9 Cockroft-Walton type high voltage power supplies (CW-HVPS) so that each EC can be powered independently. A detailed description of the power supply is given in [7]. The 36 MAPMTs were sorted before the assembly of the PDM to gather MAPMTs with similar gain in the same EC. The ECs are potted to avoid disruptive discharge due to high voltage when flying at  $\sim 3 \text{ mbar}$  in the stratosphere.

A Schott UV BG3 1 mm thick band filter (290-430 nm) is glued on each MAPMT's window glass to increase the signal-to-noise ratio. The sides of the filter are beveled to act like a light guide and reduce the dead space between the MAPMTs.

The  $64 \times 36$  channels are read by 36 SPACIROC I ASICs<sup>1</sup> [8]. Those ASICs have 64 photon counting channels that are able to perform single photoelectron detection. Each of the 64 channels

<sup>1</sup>Application Specific Integrated Circuit

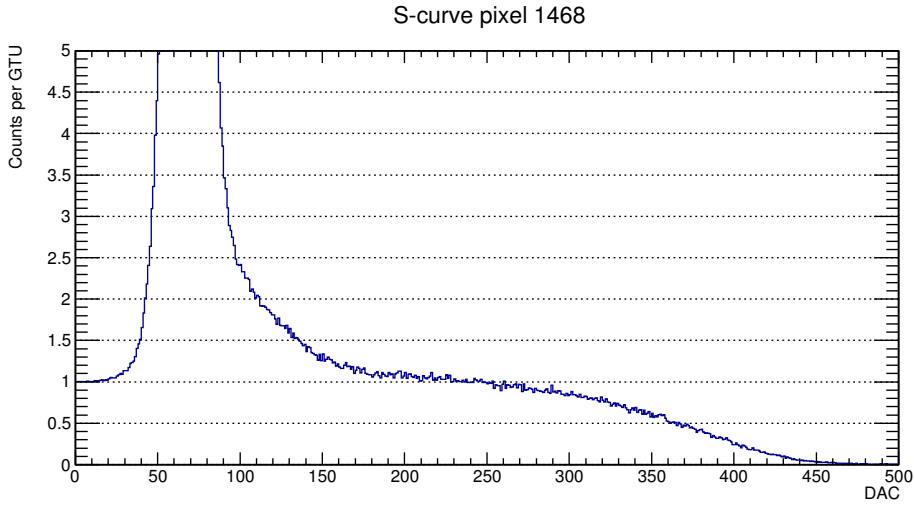


**Figure 1:** S-curve of one channel out of the 2,304 of EUSO-Balloon. The truncated left peak represents the saturated integration of the electronic noise : the ASICs present a paralyzable dead time of 30 ns so that number of counts fall to 1 when all signals arrive with less than 30 ns intervals. The number of counts on the plateau region represents the mean number of photoelectrons counted per GTU (2.3  $\mu$ s). The mean of the single photoelectron peak is represented by the inflexion point of the curve around DAC 380. More than 10,000 GTUs are acquired in this curve to get a statistical error in  $1/\sqrt{N}$  of less than 1%.

signals are preamplified with an 8-bit gain adjustment (a factor from 0 to 4). The signals are discriminated with a 10-bit DAC register comparator to count the single photoelectron pulses. The counts are integrated by time windows of 2.3  $\mu$ s called Gate Time Unit (GTU).

An example of an integrated single photoelectron spectrum registered with SPACIROC I ASIC and the flight model DAQ of EUSO-Balloon [10] is presented in figure 1. It is acquired by changing the DAC threshold of the discriminator and represents then the number of counts above the threshold. This type of curve is referred to as S-curve.

### 3. Calibration of the Photo-Detector Module

To measure the UV background with the EUSO-Balloon instrument, a precise calibration of the instrument is needed. The calibration of the PDM at a 950 V photocathode voltage for the 378 nm wavelength is presented in the following section. The reason of this precise value is explained in section 4. The calibration is needed to know the detection efficiency which is defined as:

$$\varepsilon(\lambda, V, \text{DAC}) = \varepsilon_{\text{filter}}(\lambda) \times \varepsilon_{\text{quantum}}(\lambda) \times \varepsilon_{\text{collection}}(V) \times \varepsilon_{\text{threshold}}(V, \text{DAC}) \quad (3.1)$$

with  $\varepsilon_{\text{filter}}(\lambda)$  the transmission of the filter,  $\varepsilon_{\text{quantum}}(\lambda)$  the quantum efficiency of the photocathode,  $\varepsilon_{\text{collection}}(V)$  the collection efficiency of the PMT, which corresponds to the probability that a photoelectron emitted by the photocathode is collected on the first dynode. It depends on the strength of the electric field between the photocathode and the first dynode.

The last parameter  $\varepsilon_{\text{threshold}}(V, \text{DAC})$  represents the probability that a photoelectron will have an amplitude high enough to be selected by the threshold of the comparator. If the gain of a PMT

is too low, the signal amplitude is too low to be distinguishable from the electronic noise. The few signals selected by the threshold will then lead to a low  $\epsilon_{\text{threshold}}$  factor.

The calibration has been processed using the technique developed by Lefeuvre and Gorodetzky which uses a calibrated reference detector instead of a calibrated source of light [9]. The reference detector is a NIST photodiode with a pico-ammeter that converts current into a power by applying automatically the NIST efficiency calibration factor in function of the wavelength. The power is measured with a 1.5 % accuracy. A 378 nm LED is mounted to an integrating sphere to match the gain of the NIST photodiode ( $\sim 1$ ) that measure the light flux and the gain of the MAPMTs ( $\sim 10^6$ ). This technique has been already used in [11] to sort MAPMTs by their gains. The main difference here is that the flight DAQ is used to read the 2,304 pixels of the PDM is possible in  $\sim 1$  hour with the statistics as in figure 1.

The calibration is processed in a dedicated black box in two steps:

- A few pixels in each MAPMT are absolutely calibrated.
- The rest of the PDM's pixels are relatively calibrated with respect to the reference pixels.

The calibration process of reference pixels has already been presented in [12] where a charge ADC is used contrary to the flight model DAQ used in this present work. Thereby, the calibration of reference pixels is performed with an accuracy better than 3%. One must take care of the possible pile-up of photoelectron events due to the non-negligible 30 ns paralysing dead time of the ASICs. The maximum rate of events per integrating window to prevent a pile-up rate of more than 1% is computed by using Poisson's statistics.

The detection efficiency of the rest of the PDM is measured relative to the reference pixels. The integrating sphere being a Lambertian light source, each EC of the PDM is illuminated with a uniformity better than 1% if it is placed about 40 cm from it (the dimensions of the black box used for the calibration are not big enough to illuminate the whole PDM). By simply comparing the number of counts for each pixel to the number of counts of the reference pixels, the detection efficiency of the whole EC-unit can be obtained. The accuracy on the measurement is better than 5% for the EC-units that have the highest gain.

For all pixels a total of  $N \simeq 10,000$  GTUs at an illumination flux of 1 photoelectron per GTU is performed to maintain statistical error in  $1/\sqrt{N}$  below 1%.

#### 4. Results of the calibration

The efficiency map of the PDM measured after the flight is shown in figure 2. The efficiency fluctuations are due to the polarization voltage 950 V used which is too low for some of the EC-units. A defect in the insulation of the EC-units prevented applying a photocathode voltage higher than 950 V when flying at 38 km altitude under 3 mbar atmosphere. With this pressure condition, insulation constraints are the highest that can be encountered. For example, two electrodes at a 1000 V differential potential need to be separated by  $\sim 5$  cm at 3 mbar rather than a millimeter that is sufficient at 1 bar.

In terms of detection efficiency and its associated uncertainty, MAPMTs have been classified for the specific uses in function of the EUSO-Balloon mission criteria. Pixels presenting highest

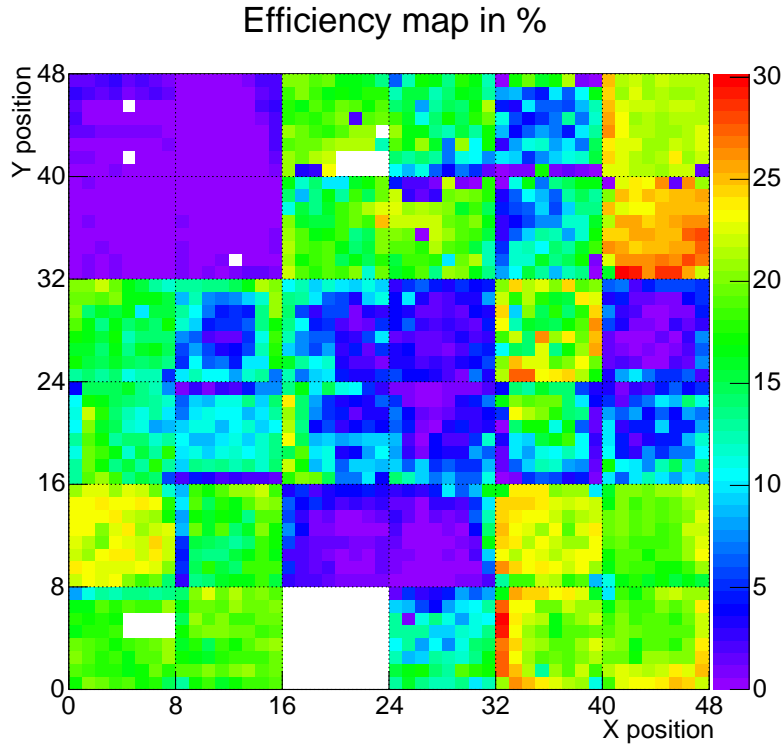


**Figure 2:** Efficiency map of the PDM at 950 V. The X- and Y-axis represent the position of the pixels and the color scale the efficiency expressed in percentage.

efficiency and lowest uncertainty are used for UV background measurement. The fact that the whole PDM is not used for this application does not penalize the quality of the measurements as a simple line can monitor the overflow areas in the manner of a scanner used to digitize a paper document. Those good pixels being in the corners, the slow rotation of the instrument following the nadir axis allows also the full observation of the area overflow and present in the field of view.

Pixels with a lower gain (and thus detection efficiency) and a higher uncertainty are used to detect UV tracks induced by laser shots. Those events are used to test the trigger algorithms [13] and are bright enough to be detected by most of the pixels. The reconstruction of the geometry of the laser tracks [2] is possible with those kind of pixels. Their low efficiency has no impact on the time information needed for the reconstruction. However, pixels with efficiencies much lower than 5% can hardly detect light from those high luminosity events. The white pixels represents ASICs with defects in the digital transmission of the data.

Calibration results before and after flight have been compared to check for possible differences in gain and efficiency. Those differences could be due to, for example, the ageing of MAPMTs after the overfly of bright UV sources, like cities. For the next flights, an active bright sources protection will be implemented. By decreasing the voltage on the photocathode, and thus the collection efficiency of MAPMTs, anode current is kept below the limit recommended by Hamamatsu. The switch voltage on the photocathode is driven by the ASIC with a reaction time equal to the GTU.

It has been discovered that the observed gain of 6 MAPMTs read by the same front-end elec-

tronics board presented large increase after the flight. This problem is due to some electronics issues in the board and those pixels are not used to reconstruct the UV intensities. However their timing information can still be used for the geometrical reconstruction of the laser induced UV tracks.

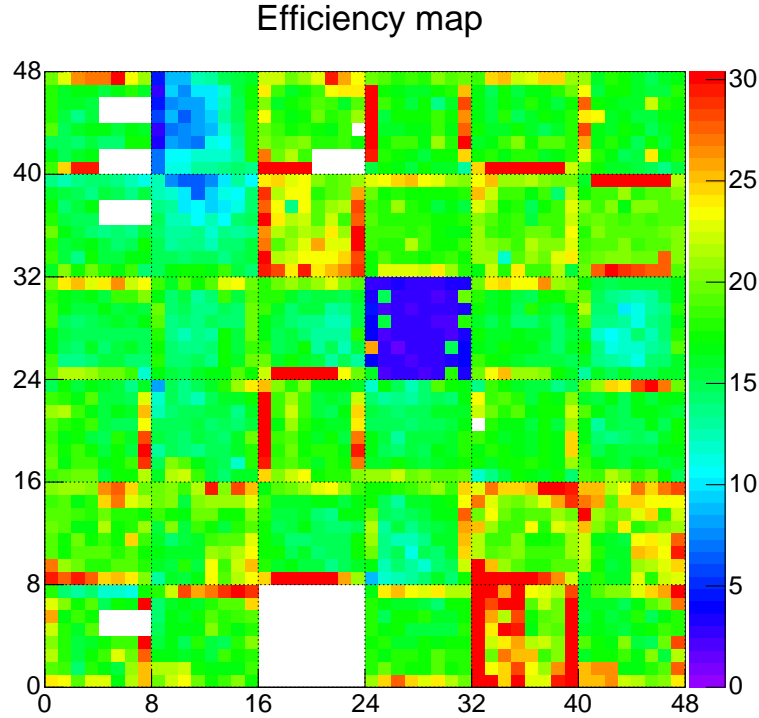


**Figure 3:** Efficiency map of the PDM at 1100 V. The X- and Y- axis represents the position of the pixels and the color scale the efficiency expressed in percentage.

## 5. Improvements for futures missions

Once the defect of insulation of the ECs is corrected, the PDM would operate properly at 1100 V at 3 mbar. The measurement of the efficiency of the PDM at 1100 V and 1 atm is presented in figure 3. It can be compared to the efficiency map measured at 950 V in figure 2. It can be seen that this increase in voltage is translated into a standardization of the efficiency of the PDM. Almost all MAPMTs that presented low gain at 950 V and thus low detection efficiency are recovered. This is due to the fact that the factor  $\epsilon_{\text{threshold}}(V, \text{DAC})$  increases, the signal-over-noise ratio is stronger. The white square of  $8 \times 8$  pixels corresponds to a defective ASIC. The other white rectangles are data transmission errors. The borders of the MAPMTs show a higher efficiency due to the light guide effect of the UV filter. Thus those pixels have a higher surface compared to pixels in the center.

## 6. Conclusion

The calibration of the PDM of EUSO-Balloon has been performed to measure the detection efficiency with an accuracy of  $\sim 5\%$  for the MAPMTs presenting the highest gains. MAPMTs used to measure the UV background over a variety of lands and cloud conditions. Pixels presenting a lower gain/efficiency are used in addition to high gain pixels to register the UV tracks induced by laser shots from a helicopter. The identification of the defect preventing to power MAPMTs up to 1100 V has been identify and is fixable. The measurements made on ground at this voltage level show that more than 95% of the active MAPMTs (the one read by a defective ASIC is not taken into account) present a high detection efficiency. Future flights will use a full PDM with maximum detection efficiency available with this type of device.

## References

- [1] J.H. Adams *et al.*, *An evaluation of the exposure in nadir observation of the JEM-EUSO mission*, *Astroparticle Physics* **44** (2013) 76 [astro-ph.HE/1305.2478].
- [2] J. Eser *et al.*, *Laser reconstruction in EUSO-Balloon experiment*, in proceedings of the 34th ICRC, PoS (ICRC2015) 0860.
- [3] Š. Mackovjak, *Night time measurement of the UV background by EUSO-Balloon*, in proceedings of the 34th ICRC, PoS (ICRC2015) 1302.
- [4] C. Catalano, *Performance of the EUSO-Balloon optics*, in proceedings of the 34th ICRC, PoS (ICRC2015) 0717.
- [5] P. von Ballmoos, *General overview of EUSO-Balloon mission*, in proceedings of the 34th ICRC, PoS (ICRC2015) 0725.
- [6] M. D. Rodríguez Frías, *The Infrared Camera onboard the EUSO-Balloon (CNES) flight on August 24, 2015*, in proceedings of the 34th ICRC, PoS (ICRC2015) 1309.
- [7] P. Gorodetzky, *A Cockcroft-Walton High-Voltage Power Supply for the EUSO Instruments*, in proceedings of the 34th ICRC, PoS (ICRC2015) 1364.
- [8] S. Ahmad, *SPACIROC: A Front-End Readout {ASIC} for JEM-EUSO Cosmic Ray Observatory*, in proceedings of the 2nd International Conference on Technology and Instrumentation in Particle Physics (TIPP 2011), *Physics Procedia* **37** (2012).
- [9] G. Lefeuvre, *Measurement of the absolute fluorescence yield in Nitrogen between 0.5 and 2.3 MeV*, in proceedings of the 29th ICRC, *International Union of Pure and Applied Physics* **8** (2005).
- [10] G. Osteria, *The Data Processor System of EUSO Balloon: in flight performance*, in proceedings of the 34th ICRC, PoS (ICRC2015) 1025.
- [11] C. Blaksley, *Photomultiplier Tube Sorting for JEM-EUSO and EUSO-Balloon*, in proceedings of the 33rd ICRC, contribution number 0628.
- [12] P. Gorodetzky, *Absolute calibrations of the Focal Surface of the Jem-Euso Telescope*, in proceedings of the 33rd ICRC, contribution number 0858.
- [13] G. Suino, *Tests of JEM-EUSO 1st level trigger using EUSO-Balloon data*, in proceedings of the 34th ICRC, PoS (ICRC2015) 0925.